Developments in NDT for Detecting Imperfections in Friction Stir Welds in Aluminium Alloys

Telmo Santos, Pedro Vilaça*, Luísa Quintino

Technical University of Lisbon, IST, Secção de Tecnologia Mecânica, Av. Rovisco Pais, 1049-001 Lisbon, Portugal
* Corresponding author: pedro.vilaca@ist.utl.pt

Abstract
Friction stir welding (FSW) has dramatically changed how aluminium alloys can be welded. The quality of FS welds is usually excellent, but some imperfections periodically occur. The geometry, location, and microstructural nature of these imperfections bear no resemblance to the imperfections typically found in aluminium fusion welds. Consequently, it has been difficult to identify FS weld imperfections with common non-destructive testing (NDT) techniques. Therefore, further development of NDT techniques must be done to enable the detection of FS weld imperfections. This paper presents an integrated, on-line, NDT inspection system for FS welds, which employs a data fusion algorithm with fuzzy logic and fuzzy inference functions. It works by analyzing complementary and redundant data acquired from several NDT techniques (ultrasonic, Time of Flight Diffraction (ToFD), and eddy currents) to generate a synergistic effect that is used by the software to improve the confidence of detecting imperfections. The system was tested on friction stir welded AA5083-H111 specimens. The results indicate that by combining the output from various NDT processes, an improvement in finding imperfections can be obtained compared to using each NDT process individually. The methodology implemented in the QNDT_FSW system has given good results and improved reliability in the NDT of friction stir welds.

Key words: *Friction Stir Welding, Non-Destructive Testing, Imperfections, Data Fusion, AA5083-H111.*

1. INTRODUCTION

1.1. The FSW process and quality assessment in FSW applications

FSW is emerging as a key technology in many industrial applications, especially those involving the joining of light alloys, such as aluminium [1], [2]. The increased application of these materials, primarily by large companies and by very demanding industrial sectors, e.g., aerospace, naval, and automotive [3], has generated significant research and development in FSW. The industrial environment in which FSW is applied demands fast (on-line, if possible) and cost efficient non-destructive testing (NDT) of welds. But, due to the solid state nature of FSW, many of the resulting weld imperfections are different than those found in fusion welds, e.g., inclusions, volumetric imperfections, and undercut. Instead, many imperfections are of a metallurgical nature and cannot be identified with typical NDT techniques [4], [5]. Because the quality of FS welds impacts manufacturing cost and product quality, appropriate quality control should be implemented to detect imperfections in friction stir welds. Since there are no universally accepted quality assurance procedures for friction stir welds, they need to be developed and incorporated into industrial, national, and international standards.

1.2. Typical imperfections of FSW

FS welds are usually free of imperfections. However, some imperfections may arise due to improper stirring of the parent material, inadequate surface preparation, lack of penetration of the pin, or inadequate axial forging forces. Some typical FS weld imperfections include lack of penetration (incorrectly called "kissing-bond"), root imperfections (weak or intermittent welding), cavities on the advancing side of the weld, and second phase particles and oxides aligned under the shoulder (Fig. 1) [4].

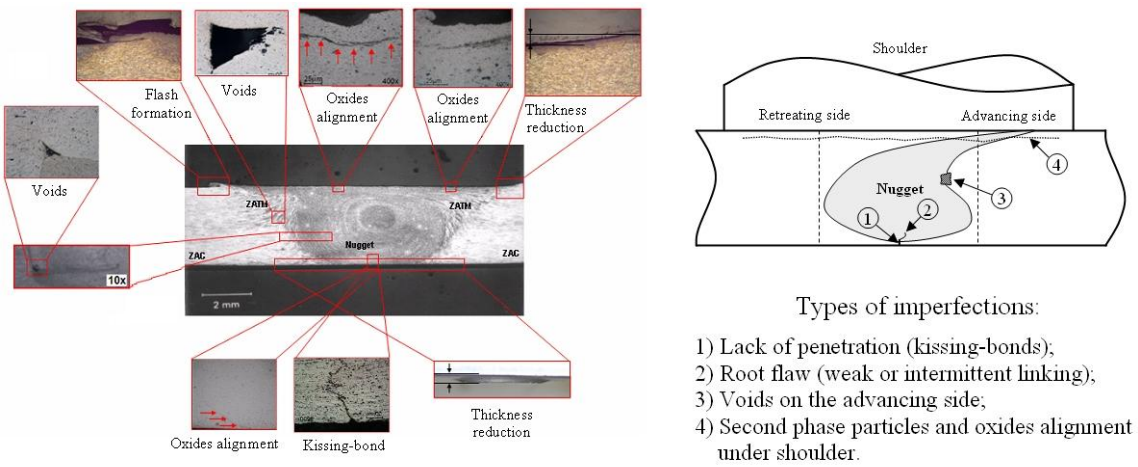

Fig. 1 – Typical imperfections in FS welded butt joints

Table 1 summarises these imperfections in terms of location, process parameters, and related conditions.

Table 1 – Description of typical FS weld imperfections

Local	Assignment	Description
Imperfections on the root of the bead	Lack of penetration	Incomplete in depth processing of the material below the pin of the FSW tool. Typically it occurs when the pin length is less than the thickness of the parent material. The materials are in close contact, but are not chemically or mechanically bonded (kissing-bond).
	Root flaw	The dynamically recrystallized zone fills the total thickness of the joint, but there are still some second phase particles and/or oxides aligned from the root of the joint into the nugget, in a more or less continuous path.
Imperfections in the interior of the weld	Cavities	Anomalous, visco-plastic flow of the material around the pin. This imperfection typically results from a bad choice of the FSW tool geometry and process parameters, in relation to the base material's thermo-physical properties.
	Second phase particles and aligned oxides	Second phase particle alignment can be found in many locations in the nugget and depends a lot on the geometry of the FSW tool, including both shoulder and pin. One of the typical locations is in the zone processed by the shoulder becoming the top surface of the weld and highlighting the true sliding interface.

1.3. NDT developments for FSW

In general, the data available on the application of NDT to FS welds is scarce [4]. Nevertheless, many projects were begun to study this subject, e.g., QUALISTIR (European consortium project involving Research and Technology Development entities) [6] and special eddy-currents probes such as Meandering Winding Magnetometer (MWM^{TM}) (developed in the USA by the consortium comprised of JENTEK Sensors, Lockheed Martin and NASA) [7]. These projects are pushed by industry's total quality management concepts, which are based on very high quality standards and total quality assurance paradigms. The aeronautics industry imposes the most stringent quality requirements one can find.

Moreover, the typical NDT techniques, such as, visual inspection, magnetic particle inspection, dye penetrant inspection, and radiographic inspection, do not enable the detection or quantification of typical FSW imperfections [5]. Ultrasound and eddy-current NDT processes, even in their most evolved form, e.g., ultrasonic phased array and eddy current array, although allowing the detection of most of the imperfections in the weld, are very sensitive to coupling and lift-off conditions between the probes and the surfaces under inspection. None of these NDT techniques, in a standalone condition, allow the assessment of the morphological diversity and localisation of all FSW imperfections [4]. Thus, the need for a data fusion algorithm [8], [9], specifically developed for the NDT of FS welds, is mandatory.
A new, specific data fusion algorithm will be presented in this paper. This innovative approach, which was specifically developed for the NDT of FS welds, is based on fuzzy logic and fuzzy inference functions to create a powerful fusion of NDT data. This data fusion methodology has many advantages when compared to the conventional Dempster-Shafer evidence theory (DSET) or Bayesian inference approaches [4].

2. INTEGRATED NDT SYSTEM FOR FSW: *QNDT_FSW*

The Quantitative Non Destructive Testing for FSW (QNDT_FSW) is an integrated, on-line system. It employs a data fusion algorithm to improve the confidence of inspection based on Relative Operating Characteristics (ROC) and Probability of Detection (PoD). The

complementary and redundant data acquired from several NDT techniques generate a synergistic effect, which is the main advantage of the present approach. The data fusion algorithm uses fuzzy logic and fuzzy interference functions to mingle the data from several NDT techniques.

2.1. Experimental set-up

The QNDT_FSW system incorporates three, distinct NDT techniques. They include a 4 MHz creeping ultrasonic probe, a 15 MHz Time of Flight Diffraction (ToFD) probe, a 20 kHz eddy current probe, and a 2 MHz eddy current probe [4]. These techniques were selected to detect, as much as possible, the position and diversity of imperfections in FS welds [5] (Table 2).

Table 2 – NDT technique guide for various types of imperfections

Imperfections \ NDT		*Creeping* + Attenuation (Side A)	*Creeping* + Attenuation (Side B)	ToFD	Eddy currents (Low freq.)	Eddy currents (High freq.)
On the root of the weld	Lack of penetration	✓	✓	✓	✓	✓
	Root flaw				✓	✓
Imperfections in the interior of the weld	Cavities	✓	✓	✓	✓	
	Second phase particles and aligned oxides	✓	✓			

The probes were used to examine the root surface of the weld because it was the smoother surface. The root is also where the superficial imperfections in FSW are the most critical [2]. Creeping ultrasonic inspection was performed on both retreating and advancing sides of the weld, where the insonification direction was always perpendicular to the welding direction (see Figure 3). Gathering data from both sides of the weld created a redundancy of data, which was analyzed by the data fusion algorithm.
Moreover, creeping inspection was complemented with data that came from attenuation measurements. The measurement of the attenuation is performed with an ultrasonic probe working in receiving mode, located at the opposite side of the weld bead in the same insonification plane of the creeping probe. Therefore, in the case of an imperfection, a creeping signal change occurs along with increasing attenuation. These two, simultaneous conditions allowed the data fusion algorithm to distinguish between signal disturbance and real imperfections.

The probes were incorporated into a mechanical support system that allowed the entire length of the weld to be analyzed in one, longitudinal pass. Fig. 2 shows the laboratory apparatus that was used to perform the NDT inspection.

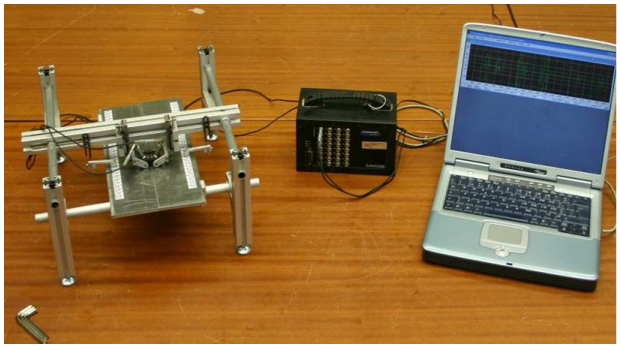

Fig. 2 – Laboratory apparatus for inspecting FS welds: the mechanical support system device and the computational data acquisition device

The QNDT_FSW system was developed for automatic, on-line inspection of welds. Critical variables for inspection included pressure, distance, and position of the probes relative to the weld root. Fig. 3 shows the fixture device and motion system device that created constant, operating conditions along the weld.

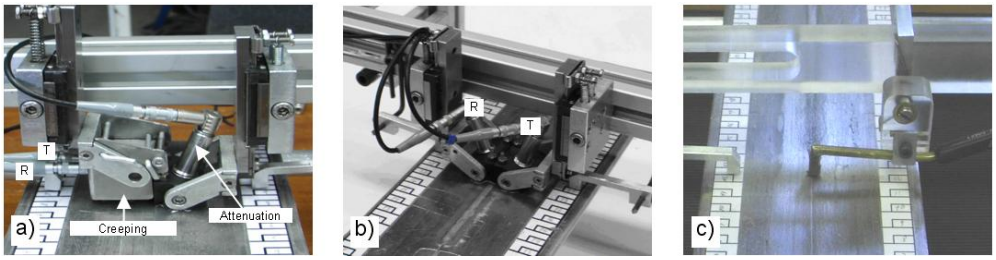

Fig. 3 – NDT probes and motion devices
a) Creeping and attenuation probes b) ToFD probes c) Eddy currents probes (T-Transmitting probe, R-Receiving probe)

The position of the probes along the weld was selected to avoid the interaction of ultrasonic and electrical fields (Fig. 4a). Moreover, the probes' transverse position assured complete and redundant coverage of the entire cross-section of the weld (Fig. 4 b).

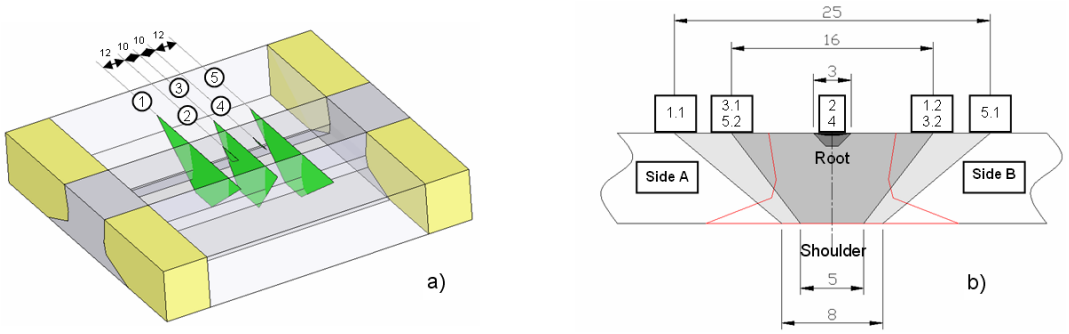

1.1 – Creeping side A;
1.2 – Attenuation measurement from side A;
2 – Eddy currents low frequency;
3.1 – ToFD emission;
3.2 – ToFD reception;
4 – Eddy currents high frequency;
5.1 – Creeping side B;
5.2 – Attenuation measurement from side B;

Fig. 4 – Longitudinal and transverse probes' position
a) Longitudinal position b) Transverse position

2.2. QNDT_FSW algorithm description

The QNDT_FSW integrated data fusion algorithm involved 5 distinct stages.

Stage 1 – NDT data acquisition: the data acquired from each of the 6 probes was saved in a file that contained the points of the inspection curve for each weld bead cross-section that was inspected.

Stage 2 – Features extraction: the curves undergo numerical signal processing to calculate the characteristic matrix of variables. This matrix numerically represents the properties of interest of the curves. These properties of interest are the ones commonly used by NDT experts to assess the weld quality, such as local maximums, distance between maximums, echoes and sound diffractions integrals, modulus and argument of the electrical complex impedance. For each weld section, the 13 characteristic variables established in Table 3 were calculated. They were then arranged in a matrix format. For the present application, 13 characteristic variables were calculated, resulting in a 13 x N matrix, where N is the number of inspected weld sections.

Table 3 – Establishment and description of the 13 characteristic variables, CV_i, representing the selected properties of interest of each of the NDT techniques data

NDT			CV_i	Description	Behavior	
					Without defect	With defect
Ultra-sons	Side A	Creeping	1	Trapezoidal integral of the first echo	↓	↑
			2	Trapezoidal integral of the second echo		
		Attenuation	3	Sum of the trapezoidal integrals of the extreme echoes module	↑	↓
	Side B	Creeping	4	Trapezoidal integral of the first echo	↓	↑
			5	Trapezoidal integral of the second echo		
		Attenuation	6	Sum of the trapezoidal integrals of the extreme echoes module	↑	↓
ToFD			7	Multiplication of the trapezoidal integral of the diffracted wave and the maximum module of this wave		
			8	Multiplication of the trapezoidal integral of the diffracted wave and the maximum module of this wave	↓	↑
			9	Sum of the trapezoidal integrals of the modules of the back waves longitudinal and transverse	↑	↓
Eddy	Low frequency		10	Electric impedance modulus	↓	↑
			11	Electric impedance phase		
	High frequency		12	Electric impedance modulus		
			13	Electric impedance phase		

Stage 3 – Fuzzification of the characteristic variables matrix: the characteristic variables were fuzzified using a membership fuzzy function that was dynamically parameterized according to the two, extreme conditions used to calibrate the system (an imperfection-free standard and a high imperfections standard).

Stage 4 – Data fusion: for each weld bead section, the data were mingled by two fuzzy interference functions that created the root imperfection index (RII) (Eq. 1) and the internal imperfection index (III) (Eq. 2). These functions were calculated using 3 types of fuzzy aggregation operators [10]: conjunctive operators ($\otimes$ - t-norms), compensatory operators ($*$ - generalized means), and disjunctive operators ($\oplus$ t-conorms). In the present application, for

both RII and III, the choice of the fuzzy characteristic variables μ_i, and the types of fuzzy operators and functions hierarchy, were selected according to criteria that were related to the NDT of FS welds [4].

$$RII = [(\mu_1 * \mu_4) \oplus (\mu_7 \otimes \mu_9)] * [(\mu_{10} \oplus \mu_{11}) * (\mu_{12} \oplus \mu_{13})] \quad (1)$$

$$III = [((\mu_1 * \mu_4) * (\mu_2 * \mu_5)) * (\mu_3 * \mu_6)] \otimes [(\mu_7 \otimes \mu_9) \oplus \mu_8] \quad (2)$$

Stage 5 – System output: the output was the RII and III of each weld cross section. This imperfection index varied in the *Imperfection-free standard* (0% imperfections) and *High imperfection standard* (100% imperfections).

The system allowed the imperfection detection process to be done automatically, without the need for a high level of NDT expertise. A graphical user interface enabled simple access to all results and the evolution of the imperfection index is graphically represented for the acquired weld sections.

3. APPLICATION OF THE QNDT_FSW

To test the QNDT_FSW system, some friction stir welds were made on 7 mm thick AA5083-H111 plate and then inspected.
The welds used to test the QNDT_FSW system are shown in Fig. 5. A transverse macrograph of the imperfection-free weld standard (corresponding to a bead on plate) is shown in Fig. 5a. Fig. 5b and Fig. 5c show the high-imperfection weld standard containing voids and root imperfections, respectively.

Fig. 5 – Examples of FS welds used to test the QNDT_FSW system
a) Imperfection-free standard b) High-imperfection standard c) High-imperfection standard

4. RESULTS AND DISCUSSION

Among the several FSW trials performed to validate and implement the QNDT_FSW system, two application samples are presented. The results of testing the QNDT_FSW system are presented in terms of equivalent imperfection indices called the Root Imperfection Index (RII) and the Internal Imperfection Index (III). These imperfection indices were calculated with the fusion inference functions (Eqs. 1 and 2) and represent the data fusion result for all of the NDT techniques used (Table 2) to examine each weld section. An imperfection index equal to 100 % means a high-imperfection weld section, similar to the high-imperfection weld standard. An imperfection index equal to 0 % means an imperfection-free weld section, similar to imperfection-free weld standards (Fig. 5). The QNDT_FSW system allows one to

set a critical level for the defect index because typical structural applications are allowed to contain defects up to a certain critical size. A 30 percent defect index was used for all cross-sections in all samples.

Fig. 6 presents the results of applying the QNDT_FSW system to 3 different FSW trials. The trials were performed with a pin length of 6.8 mm, a tilt angle of 2º, and a rotation speed of 710 rpm. The difference between these 3 trials was a change in the travel speed. In section 11 to section 1, the travel speed was 160 mm/min; from section 21 to section 12, the travel speed was 224 mm/min; and from section 34 to section 22, the travel speed was 320 mm/min.

Based on a comparison (see Figure 6) of the RII and III results with the macroscopic, visual, and radiographic test results, the following conclusions were made:
– The exit holes located at sections 1, 12 and 22 were detected by both imperfection indices;
– In section 8, the III revealed a cavity, which was corroborated by radiographic testing and visual inspection as the cavity breaks the surface of the workpiece. Moreover, the RII was not affected, which confirmed the independence of both imperfection indices;
– Sections 14 to 18 present a very low III, which was corroborated by radiographic testing. RII was able to detect small, root imperfections, as confirmed by metallographic cross-sections of the weld. Emphasis should be given to the fact that in these sections, radiographic testing cannot detect a root imperfection;
– For the 3 FSW trials, the RII increased as the travel speed increased. This behaviour was expected because the pin length was 0.2 mm shorter than the plate thickness. This created a small root imperfection that increased with increased in size as the travel speed increased.

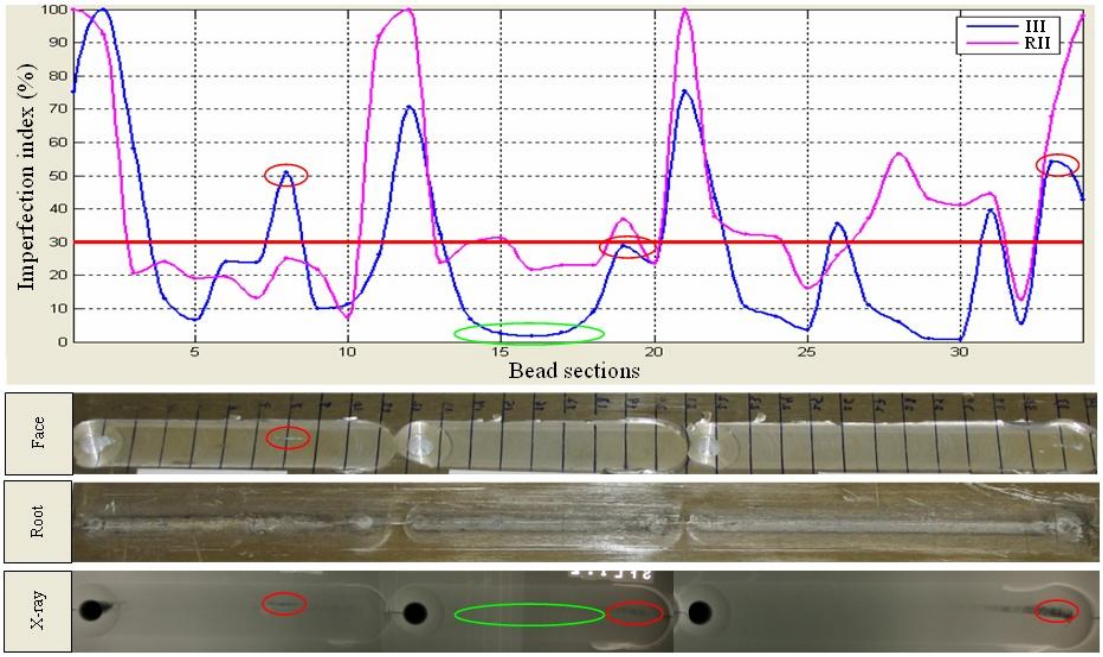

Fig. 6 – RII and III for three consecutive welds: First application sample

Fig. 7 presents the results of applying the QNDT_FSW system to sample 2. In this application, 3 different FSW trials were performed with Tool 3, a tilt angle of 2º, a rotation speed of 710 r/min, and a travel speed of 160 mm/min (Table 3). The difference between these 3 trials is the pin length, where from section 1 to section 12 the pin length was 5 mm;

from section 13 to section 22, the pin length was 6 mm; from section 23 to section 30, the pin length was initially 6.8 mm, but at section 26, the pin broke, as can be confirmed in the radiographic analysis, and thus, from then on, the pin length was zero.

Once again, the RII and III results from QNDT_FSW system were compared with macroscopic analysis and visual analysis of the top and root surfaces of the weld and with the results of radiographic tests. Again, the results accurately predicted the quality of the weld. In fact, Fig. 7 shows a high RII along all weld sections. The results from the existing root flaw can be seen in Fig. 8. This root flaw was intentionally produced by using pin lengths shorter than the 7mm thick plate, which resulted in lack of penetration of the weld. Even these large root flaws were not detected by the radiographic testing. The RII reflected the exit holes at the end of the weld. The RII was sensitive enough to detect the internal imperfections in sections 1 to 5, and the unwelded portion of the plate, after the pin broke at section 26.

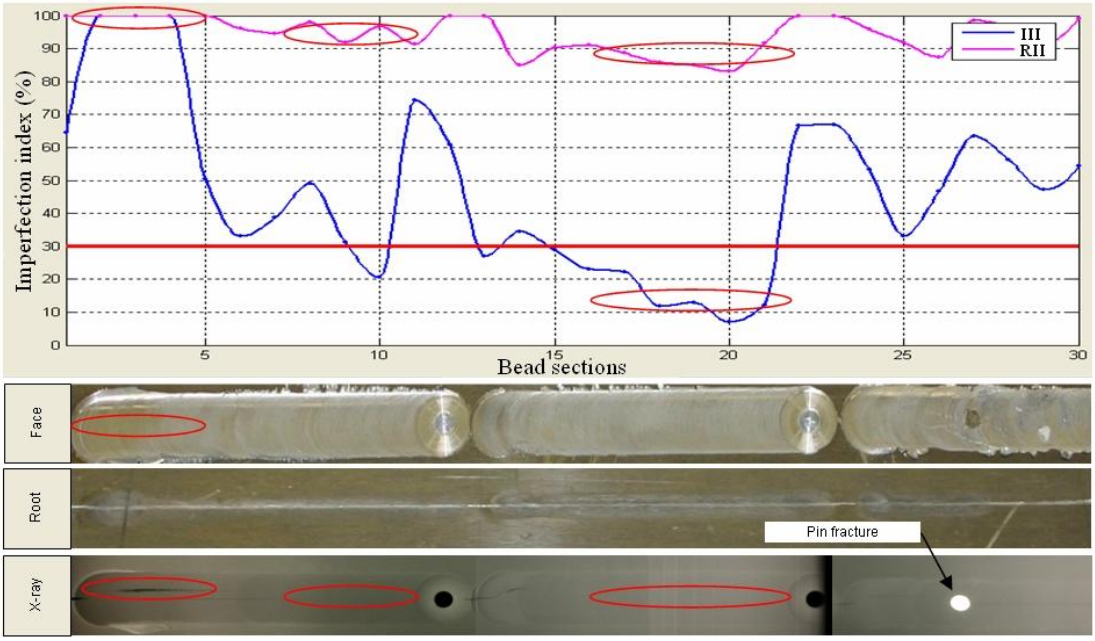

Fig. 7 – RII and III for three consecutive weld beads: Second application sample

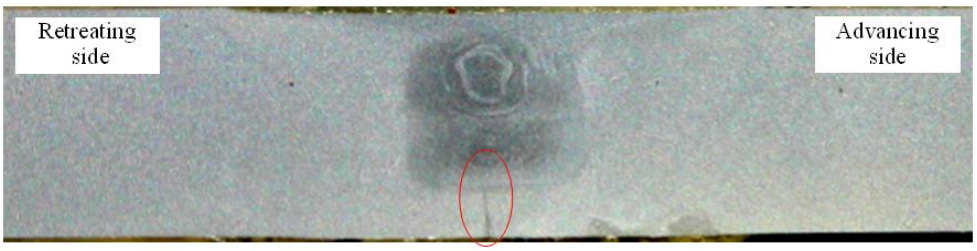

Fig. 8 – Macrograph of section 15 of the second application sample trials. Note the large root flaw due to incomplete penetration of the FSW tool

4.1. Evaluation of the synergic effect of the algorithm

The present analysis will allow to address benefits of the synergic effect of the data fusion of the different techniques. A comparison between III and RII is done with the result obtained when using the NDT characteristic variables μ_i before data fusion. The aim is to evaluate the

reliability level of using the imperfection indexes III and RII compared to each technique separately.

For the first application sample, Fig. 9a) shows the comparison between III and the characteristic variable μ_1 (niu1), which means the trapezoidal integral of the first creeping echo. It can be observed that μ_1 alone doesn't indicate the defects in the interior of the weld as accurately as the internal imperfection index (III), namely in sections 13 to 17, where the internal detect is significantly smaller than the size suggested by μ_1.
For the second application sample, Fig. 9b) shows the comparison between RII and the characteristic variable μ_7 (niu7), which means the maximum module of the diffracted ToFD wave. Once again, the variable μ_7, by itself, doesn't describe as adequately as RII the quality at the root of the weld. On sections 2 to 12 μ_7 indicates a small root detect while in reality the defect is significant as indicated by RII as discussed.
Both samples show that the characteristic variables alone do note indicate the quality status of the welds as accurately as the defects indexes. This demonstrates that the equivalent synergic indexes III and RII are more reliable than each characteristic variables by itself. Thus, the fusion data algorithm generates a beneficial synergic effect in what regards defect characterization and avoidance of conflicts.

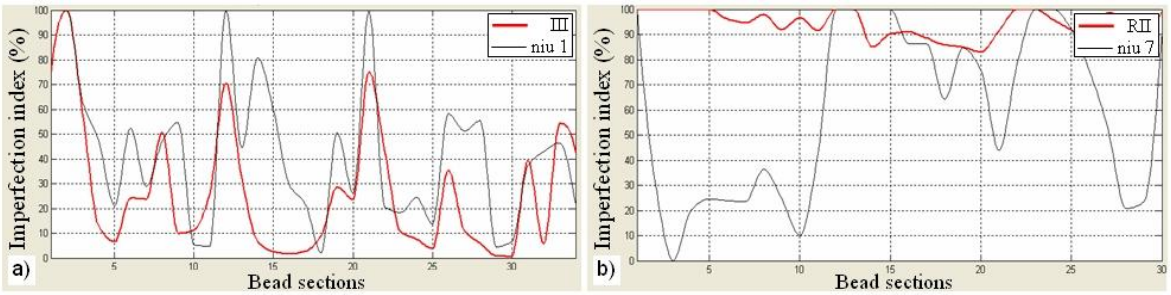

Fig. 9 – Comparison of III and RII with characteristic variables
a) Comparison between III and μ_1 (niu1) for the first application sample
b) Comparison between RII and μ_7 (niu7) for the second application sample

5. CONCLUSIONS

Several conclusions can be drawn from the development and application of the QNDT_FSW system:

An integrated NDT, data fusion system for FSW, named QNDT_FSW, was developed and tested on friction stir welded specimens;

Equivalent defect indices were proposed for evaluating the significance of root (RII) and internal (III) imperfections;

The RII and III, when compared to visual, radiographic, metallographic analysis of the face and root surfaces, confirm the feasibility in detect weld imperfections. The methodology is, therefore, a valid NDT process;

Combining the data from several NDT processes is an improvement, when compared to interpreting the individual results of each NDT process, due to the synergistic effect of the data fusion algorithm.

6. ACKNOWLEDGMENTS

The authors would like to acknowledge Fundação para Ciência e Tecnologia (FCT) for its financial support via project POCTI/EME/60990/2004 (acronym NDTStir) and the PhD scholarship FCT – SFRH/BD/29004/2006.

7. REFERENCES

[1] Vilaça, P., Pedrosa, N., Quintino, L., *Experimental Activities and Computational Developments of FSW at IST – Technical University of Lisbon*, Proceeding of Romania Welding Society (ASR), International Conference: "Welding in Romania on the Edge of Joining the European Union", Galati – Romania, 28-30th, Timisoara, pp.62-77, Set. 2005.
[2] Vilaça, P., Fundamentos do Processo de Soldadura por Fricção Linear – Análise Experimental e Modelação Analítica, PhD Thesis, IST, Technical University of Lisbon, Portugal, 2003.
[3] Vilaça, P., Quintino, L., Santos, J., Zettler, R., Sheikhi, S., *Quality Assessment of Friction Stir Welding Joints via Analytical Thermal Model, iSTIR*, International Journal of Materials Science and Engineering: A (Structural Materials: Properties, Microstructure and Processing), volumes 445-446, pp. 501-508, 15 February 2007.
[4] Santos, T., Data Fusion with Fuzzy Logic in Non-Destructive Testing of Friction Stir Welding, MSc Thesis, IST, Technical University of Lisbon, Portugal, 2006.
[5] Vilaça, P., Santos, T., Quintino, L., *Experimental Analysis, Defect Evaluation and Computational Developments of FSW*. Proceeding of IIW South East – European Regional Congress, Timisoara, Romania, 2006.
[6] Bird, R., Ultrasonic Phased Array Inspection Technology for Evaluation of Friction Stir Welds, Insight, 46, pp.31–36, 2004.
[7] Stepinski, T., *NDE of friction stir welds, nonlinear acoustics ultrasonic imaging*, Technical Report TR-04-03, Svensk Kärnbränslehantering AB, pp.3-14, 2004.
[8] Reza, H. et al., A density-based fuzzy clustering technique for non-destructive detection of defects in materials, NDT&E International, 40, pp.337–346, February 2007.
[9] Kohl, C., Streicher, D., Results of reconstructed and fused NDT-data measured in the laboratory and on-site at bridges, Cement & Concrete Composites, 28, pp.402–413, 2006.
[10] Bellman, E., Zadeh, L.; Decision making in a fuzzy environment, Management Science, v.17, n.º4, pp.141-164, 1970.